PHYSICAL REVIEW A VOLUME 32, NUMBER 1 JULY 1985

Extended coupled-channels calculations for electron-hydrogen scattering

B. H. Bransden
Department of Physics, University of Durham, Durham, England

I. E. McCarthy, J. D. Mitroy, and A. T. Stelbovics
Institute for Atomic Studies, The Flinders University of South Australia, Bedford Park, South Australia 5042, Australia
(Received 7 November 1984)

Electron-hydrogen scattering to the $1s$, $2s$, and $2p$ states is calculated at 54.42 and 200 eV, and compared with experimental data. Higher-energy reaction channels, including the continuum, are taken into account in two different ways: first, in approximate polarization potentials involving explicit integration over the appropriate kinematic degrees of freedom; second, in a set of seven pseudostates for which the 10-channel pseudoproblem is solved in full. In anticipation of larger and better pseudostate sets, approximations to the pseudoproblem are investigated. They involve second-order treatment of coupling to the pseudostates.

I. INTRODUCTION

For electron scattering on hydrogen the space of reaction channels may be divided into two by projection operators P and Q. P space includes channels to be explicitly treated by a coupled-channels calculation. Q space includes at least the target continuum. Cross sections for lower-energy excitations of states in P space converge quite quickly as more discrete channels are added. However, the continuum cannot be ignored. We consider two different ways of treating Q space in a coupled-channels calculation.

The first way is the coupled-channels optical method (CCO) developed by McCarthy and Stelbovics.[1,2] Here Q space is treated by adding a polarization potential $V_{ij}^{(Q)}$ to the potential coupling the P-space channels i,j. In practice the equivalent local polarization potential in momentum space is used. For discrete excitations it is calculated in second order with antisymmetrization. For continuum excitations the polarization potential includes the screening correlation which considerably improves the total ionization cross section (proportional to the forward diagonal imaginary polarization potential) in comparison with the second-order potential. Polarization potentials are calculated explicitly by integrating over all continuum degrees of freedom.

The CCO model is a complete *ab initio* model for all aspects of the three-body problem. Q-space aspects are treated in the Born approximation with antisymmetrization and screening. It is hoped that this will be accurate enough for calculation of P-space properties, since Q-space effects are of second order in the fully coupled calculations of P space.

The second way is to solve explicitly a pseudoproblem (PP), in which P-space channels are treated exactly but Q-space is represented by a set of normalized square-integrable pseudostates which are included in the coupled-channels calculation. In principle pseudostates can be chosen in such a way as to give a representation of the target[3] which converges as more pseudostates are added. In practical calculations up to the present limited sets of pseudostates have been chosen so as to reproduce external features of the problem. We consider the set of four s pseudostates and three p pseudostates used by Bransden, Scott, Shingal, and Roychoudhury[4] (BSSR) in a second-order optical-potential approximation to the pseudoproblem. Here the s pseudostates are similar to a set chosen by Callaway and Wooten[5] to fit low-energy s-wave phase shifts among other criteria. The p pseudostates reproduce the dipole polarizability of hydrogen.

The pseudoproblem in principle is a complete *ab initio* model for the details of P space and for the total cross section for Q space. At present we hope that the realistic set of pseudostates chosen will provide a sufficiently accurate description of second-order effects in P space and that we will obtain a guide to the use of the pseudostates to be obtained by new *ab initio* methods.[3]

An important way of using pseudostates is to construct from them polarization potentials for use in a coupled-channels calculation of P space. For example the BSSR calculation[4] uses second-order polarization potentials without exchange terms.

The present work compares calculations of CCO and PP with experiment for P space consisting of $n=1$ and 2 states. It also investigates various approximations to PP that can be used with larger pseudostate sets for which a full coupled-channels calculation is difficult.

II. MODELS OF THE ELECTRON-HYDROGEN THREE-BODY PROBLEM

The Hamiltonian for electron scattering on hydrogen is

$$H=K_1+K_2+v_1+v_2+v_3\ , \tag{1}$$

where K and v stand for kinetic-energy and potential-energy operators, respectively. Subscripts 1 and 2 label the electron-nucleus subsystems for electrons 1 and 2, respectively, and 3 labels the electron-electron system. The small kinetic energy K_3 of the nucleus is neglected. Spin-orbit coupling is neglected so that electron spin plays

a part only in considerations of antisymmetry. The total wave function is labeled by the total electron spin S which can be 0 (singlet) or 1 (triplet). The total wave function is labeled also by a quantum number n denoting the three-body state in terms of the quantum numbers of bound states and momenta of unbound electrons. It is a discrete notation for the continuum, where necessary, involving box normalization and the usual limiting processes.

The Schrödinger equation for total energy E is

$$\{E^{(\pm)}-[K_1+K_2+v_1+v_2+v_3+(-1)^S(H-E)P_r]\}\Psi_{nS}^{(\pm)} =0 , \quad (2)$$

where P_r is the space-exchange operator and the superscripts $(\pm)$ denote outgoing and ingoing spherical-wave boundary conditions, respectively. Suppressing the index S for economy of notation we use the abbreviation

$$v_3' \equiv v_3+(-1)^S(H-E)P_r . \quad (3)$$

The reaction channels are labeled by the one-electron bound-state functions ϕ_j, where j may be a discrete notation for the continuum. We choose the label 2 for the bound electron,

$$(\epsilon_j-K_2-v_2)\phi_j=0 . \quad (4)$$

We use an operator notation, where all operators are understood to act on the three-body wave function $\Psi_n^{(+)}$.

The Schrödinger equation (2) is written

$$E^{(+)}-K=v , \quad (5)$$

where

$$K=K_1+K_2 , \qquad v=v_1+v_2+v_3' . \quad (6)$$

We use projection operators P,Q for the sets P,Q of target states

$$P=\sum_{i\in P}|\phi_i\rangle\langle\phi_i| , \quad Q=1-P . \quad (7)$$

The Schrödinger equation (5) is written as two projected equations

$$P(E^{(+)}-K-v)P=PvQ , \quad (8a)$$

$$Q(E^{(+)}-K-v)Q=QvP . \quad (8b)$$

We formulate the coupled-channels problem for P space by eliminating Q space using Eq. (8b),

$$P(E^{(+)}-K-v_2-V^{(Q)})P=0 , \quad (9)$$

where $V^{(Q)}$ is the optical potential,

$$V^{(Q)}\equiv v_1+v_3'+(v_1+v_3')Q\frac{1}{Q(E^{(+)}-K-v)Q}Q(v_1+v_3') . \quad (10)$$

The last term in (10) is the complex-polarization potential.

Two possible representations for implementing the solution of the P-space equation (9) are the coordinate representation, where (9) becomes a set of coupled integro-differential equations

$$\sum_{j\in P}\langle\phi_i|E^{(+)}-K_1-V^{(Q)}|\phi_j\rangle u_j^{(+)}(\mathbf{k}_j,\mathbf{r}_1)=0, \quad i\in P \quad (11)$$

and the momentum representation, where we have a set of coupled integral equations

$$\langle\mathbf{k},\phi_i|T|\phi_j,\mathbf{k}_j\rangle=\langle\mathbf{k},\phi_i|v^{(Q)}|\phi_j,\mathbf{k}_j\rangle + \sum_{l\in P}\int d^3k'\langle\mathbf{k},\phi_i|v^{(Q)}|\phi_l,\mathbf{k}'\rangle \times\frac{1}{E^{(+)}-\epsilon_l-\frac{1}{2}(k')^2} \times\langle\mathbf{k}',\phi_l|T|\phi_j,\mathbf{k}_j\rangle . \quad (12)$$

The exact polarization potential for P-space channels i,j is written in momentum space as follows:

$$\langle\mathbf{k}'|V_{ij}^{(Q)}|\mathbf{k}\rangle=\sum_{\mu\in Q}\langle\mathbf{k}',\phi_i|v_3'|\Psi_\mu^{(-)}\rangle\frac{1}{E^{(+)}-E_\mu} \times\langle\Psi_\mu^{(-)}|v_3'|\phi_j,\mathbf{k}\rangle . \quad (13)$$

Much computational time is saved by using the equivalent local approximation[1]

$$V_{ij}^{(Q)}(P)=\tfrac{1}{2}\int_{-1}^{1}du\langle\mathbf{k}-\mathbf{k}'+\mathbf{k}_j|V_{ij}^{(Q)}|\mathbf{k}_j\rangle , \quad (14)$$

$$\mathbf{P}=\mathbf{k}-\mathbf{k}' , \qquad u=\mathbf{P}\cdot\mathbf{k}_j/Pk_j . \quad (15)$$

This approximation is used in the CCO method, together with approximations for $\Psi_\mu^{(-)}$ specified below.

The pseudoproblem can be solved directly by including all the pseudostates in P space. Alternatively BSSR[4] use a P space consisting of $1s$, $2s$, $2p_0$, and $2p_\pm$ channels (where the subscripts denote the projection quantum number) and include all the pseudostates in an optical potential. The P-space coupled equations (11) are written explicitly in atomic units as

$$(\nabla^2+k_i^2)u_i^{(+)}(\mathbf{k}_i,\mathbf{r}_1)=\sum_{j\in P}\{V_{ij}(\mathbf{r}_1)u_j^{(+)}(\mathbf{k}_j,\mathbf{r}_1)+\int d^3r_2[W_{ij}(\mathbf{r}_1,\mathbf{r}_2)+K_{ij}(\mathbf{r}_1,\mathbf{r}_2)]u_j^{(+)}(\mathbf{k}_j,\mathbf{r}_2) , \quad (16)$$

where V_{ij} and W_{ij} are the usual direct and exchange-potential matrix elements [Eq. (2)] and K_{ij} is the direct part of the second-order polarization potential matrix element

$$K_{ij}(\mathbf{r}_1,\mathbf{r}_2)=\sum_{\mu\in\bar{Q}}V_{i\mu}(\mathbf{r}_1)G_0(\tfrac{1}{2}K_\mu^2;\mathbf{r}_1,\mathbf{r}_2)V_{\mu j}(\mathbf{r}_2) . \quad (17)$$

The set of pseudostates is denoted by $\bar{Q}$ and G_0 is the free

Green's function. The models used in the present work are summarized as follows.

A. CCO

A coupled-channels calculation in momentum space is performed for P space with polarization potentials obtained from the equivalent local approximation to (13). These potentials are both diagonal and off-diagonal in the P-space channels. $\Psi_\mu^{(-)}$ is represented by the Born approximation (with exchange) for discrete excitations in Q space and by the Born approximation with screening correlation and exchange for the three-body continuum. The screening correlation means that $\Psi_\mu^{(-)}$ is approximated by the product of a plane wave for the faster electron and a Coulomb wave for the slower electron.

B. PP

The coupled equations are solved exactly for a 10-channel space consisting of the $n=1,2$ physical channels ϕ_i and the set $\bar{\phi}_\mu$ of seven pseudostates used by BSSR.[4] The space of which the $\bar{\phi}_\mu$ are elements is called $\bar{Q}$. The following approximations to PP are investigated.

BSSR: A coupled-channels calculation in coordinate space is performed for P space with polarization potentials obtained from the following approximations to the coordinate-space transform of (13). $\Psi_\mu^{(-)}$ is represented by the Born approximation without exchange for excitation of the pseudostate $\bar{\phi}_\mu$, i.e., $\bar{Q}$ space is treated in second order.

PP2: The couplings $\bar{Q}v\bar{Q}$ are omitted from the full set of couplings $(P+\bar{Q})v(P+\bar{Q})$ in a coupled-channels calculation. It has been shown by McCarthy and Stelbovics[6] that this is a coupled-channels calculation with $\bar{Q}$ space treated in second order. In order to correspond as closely as possible with BSSR, matrix elements $Pv\bar{Q}$ are computed without exchange but PvP are computed with exchange. BSSR is a polarization-potential calculation of the same approximation. Although both methods should give the same results there are relatively minor disagreements for which the reason cannot be traced.

PP2E: The same as PP2 except that the matrix elements $Pv\bar{Q}$ are computed in full, including exchange.

PSO: An approximate polarization potential (13) is used in a momentum-space calculation of P space with full coupling and exchange. In the polarization potential $\Psi_\mu^{(-)}$ is represented by the Born approximation with exchange. The polarization potential is averaged over projection quantum numbers and spherically averaged (equivalent local approximation[1]). This is an approximation to PP2E.

CC: Coupled-channels calculation for P space only.

PPD: Full coupled-channels calculation for P and $\bar{Q}$ spaces. No exchange matrix elements are included. This is calculated to assess its validity in comparison with PP, since such calculations exist in the literature.[7]

The basic models under discussion are CCO and PP. As an approximation to the $\bar{Q}$ space of PP we are mainly interested in the coordinate space second-order optical model without exchange (BSSR) and the exact second-order calculation without exchange PP2. The results of these models for 54.42- and 200-eV electron scattering are summarized in Tables I and II, in which the relevant figures for angular distributions are indicated.

At 54.42 eV there are experimental differential cross sections[8,9] and $2p$ angular correlation parameters[9–11] for comparison with the P-space features of the calculations. Apart from the total cross section σ_Q for exciting states in Q-space, only CCO gives estimates of Q-space features and these are only obtained in the Born approximation (with exchange) for discrete excitations and the Born approximation with screening and exchange for the total ionization cross section σ_I.

TABLE I. Features of the 54.42-eV e-H problem (a.u.). The columns headed Expt. and Ref. give experimental data and the corresponding reference number.

Feature	Expt.	Ref.	CCO	PP	PP2	BSSR
P space						
$d\sigma_{1s}/d\Omega$	Fig. 1[a]	8,12		Fig. 1		
σ_{1s}	3.83±0.38[a]	15	3.25	2.91	3.11	3.18
$d\sigma_{2s}/d\Omega$	Fig. 2	9		Fig. 2		
σ_{2s}	0.25±0.07[b]	9	0.251	0.167	0.131	0.124
	0.166	14				
$d\sigma_{2p}/d\Omega$	Fig. 3	9		Fig. 3		
σ_{2p}	2.79±0.24	9	2.75	2.69	2.54	2.56
λ, R	Fig. 4	9–11		Fig. 4		
Q space						
σ_Q	3.53±0.35	9,15	3.63	2.75	3.50	8.2
σ_I	2.29±0.3	16	3.1			
σ_{3s}	0.037±0.005	17	0.060			
σ_{3p}	0.34±0.04	17	0.36			

[a]50 eV.

[b]Interpolation in the angular distribution of Williams.[9]

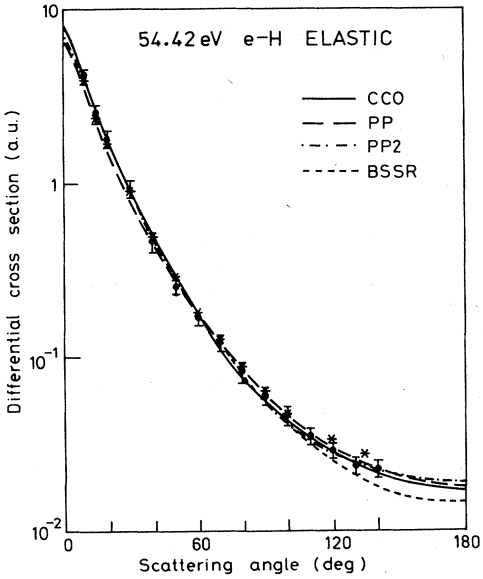

FIG. 1. e-H elastic scattering at 54.24 eV (theory) and 50 eV [experiment (Ref. 8)]. Experimental points have been multiplied by 0.82 to give a shape comparison. Experimental data are due to Williams (Ref. 8) (filled circles) and van Wingerden *et al.* (Ref. 12) (stars).

The calculation of σ_Q compares quite well with experiment for CCO at both 54.42 and 200 eV, indicating that at least this feature of the explicit polarization potential for Q space is fairly accurate. σ_I is somewhat overestimated at 54.42 eV, but is quite accurate at 200 eV.

The choice of $\overline{Q}$ space in PP to represent Q space does not give such an accurate estimate of σ_Q at either energy. PP2 does in fact give a close estimate of σ_Q at 54.42 eV, but this is only an approximation to PP and the close estimate is fortuitous. BSSR gives a surprisingly bad overestimate of σ_Q in comparison with PP2 (and experiment) at 54.42 eV, but does better at 200 eV.

CCO is the only model that gives explicit estimates of total cross sections for individual Q-space excitations. At

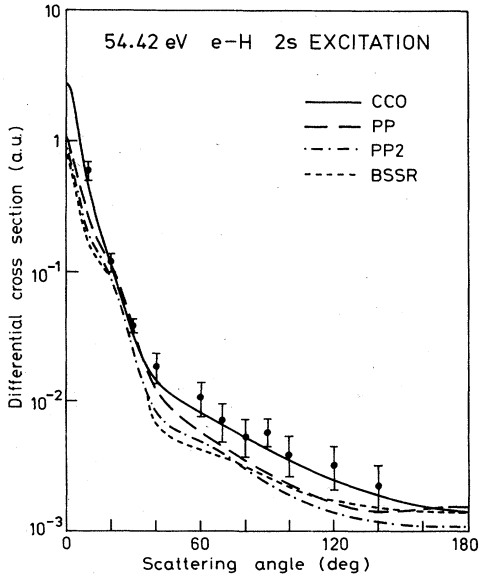

FIG. 2. e-H scattering to the 2s state at 54.42 eV.

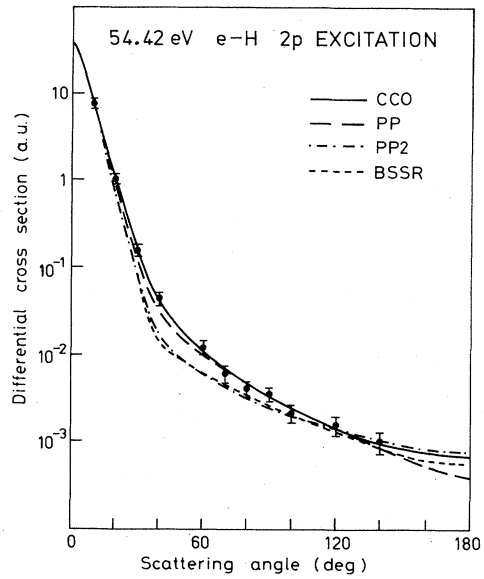

FIG. 3. e-H scattering to the 2p state at 54.42 eV. Experimental data are due to Williams (Ref. 9).

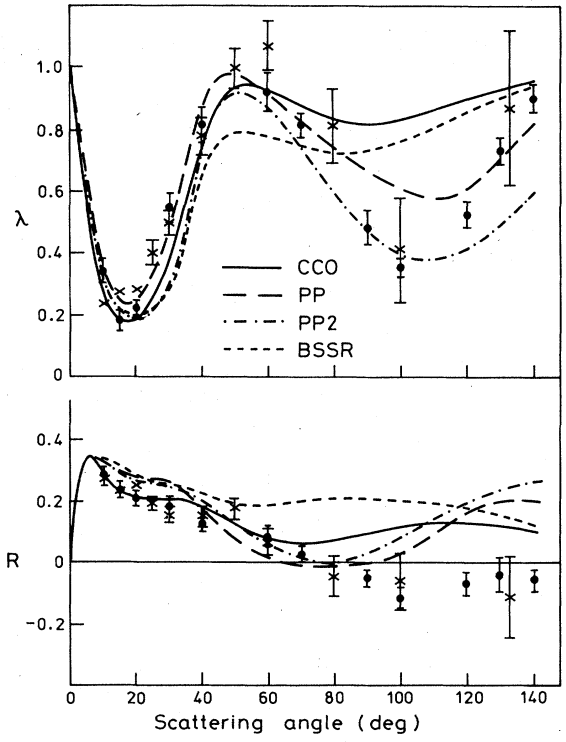

FIG. 4. 2p angular correlation parameters λ and R for the 54.42 eV e-H problem. Experimental data are due to Williams (Ref. 9) (filled circles), Hood *et al.* (Ref. 10) (crosses for θ up to 20°), Weigold *et al.* (Ref. 11) (crosses for θ beyond 20°).

TABLE II. Features of the 200-eV e-H problem (a.u.). Column headings are the same as for Table I.

Feature	Expt.	Ref.	CCO	PP	BSSR
P space					
$d\sigma_{1s}/d\Omega$	Table III	8		Table III	
σ_{1s}	0.67	15	0.60	0.59	0.58
$d\sigma_{2s}/d\Omega$				Table IV	
σ_{2s}	0.10	14	0.068	0.080	0.075
$d\sigma_{2p}/d\Omega$				Table V	
σ_{2p}	1.7	18,19	1.40	1.41	1.59
Q space					
σ_Q	2.0	14—17	1.90	1.51	1.45
σ_I	0.49±0.1	16	0.46		
σ_{3s}	0.0172	17	0.0174		
σ_{3p}	0.21	17	0.244		
$\frac{d^5\sigma^a}{d\Omega_1 d\Omega_2 dE_1}$	Fig. 5	20	Fig. 5		

[a]250 eV.

54.42 eV polarization potentials are included for $1s$-$1s$, $1s$-$2s$, $1s$-$2p$, $2s$-$2s$, and $2p$-$2p$ transitions with the intermediate states being the continuum in all cases, $3p$ and $4p$ for s-s, $3p$ and $3d$ for $1s$-$2p$, $3s$ and $3p$ for $2p$-$2p$. Here we have experimental values for σ_{3s} and σ_{3p}, which are only qualitatively estimated by the corresponding polarization potentials.

At 200 eV the explicit polarization potentials give much closer estimates of total cross sections for discrete excitations[13] (within a few percent). However, the calculation discussed here treats $3s$, $3p$, $3d$, $4s$, and $4p$ excitations by explicit coupling rather than polarization potentials. The polarization potentials are included for the same transitions as in the 54.42 eV case but involve only the continuum intermediate states. The accuracy of the $1s$-$1s$ continuum potential is shown by the excellent estimate of σ_I. The screened Born approximation even gives a qualitatively correct shape for the angular correlation in a 250-eV ionization experiment as illustrated by the example shown in Fig. 5.

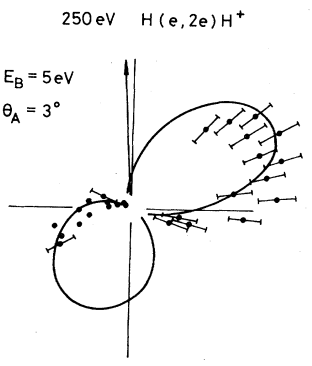

FIG. 5. Born approximation (arbitrarily normalized) to the reaction $H(e^-,2e^-)H^+$ at 250 eV. The differential cross section is plotted on a polar diagram for the slower electron (5 eV). The scattering angle of the faster electron is 3°. Experimental data are due to Lohmann *et al.* (Ref. 20).

In general CCO predicts P-space features at 54.42 eV within experimental error except for values of the angular correlation parameters λ and R beyond 80° (Fig. 4). PP predicts differential cross sections (Figs. 1—3) almost as well as CCO, except for the $2s$ excitation. Note that only the shape of the elastic angular distribution is predicted. Absolute cross sections are difficult to measure. Present experimental values[8,12] must be reduced by about 20%. PP does predict large-angle values of λ better than CCO, but the reverse is true for R, even at small angles. At 200 eV (Tables II—V) CCO and PP give essentially similar results for P-space features, usually differing by less than 10%.

III. APPROXIMATIONS TO THE PSEUDOPROBLEM

The 54.42-eV calculation has been done for all the models of Sec. II. The object is to study approximations that could conceivably be regarded as sufficient for calculating a problem involving a larger set of pseudostates for $\overline{Q}$ space. Numerical results are given in Tables VI—X.

First, the magnitude of the effect of including $\overline{Q}$ space is seen by comparing PP with the simple three-state calculation CC. The inclusion of more absorption increases the diffraction scattering at forward angles, in the elastic case (Table VI), otherwise it generally decreases cross sections for backward elastic and for inelastic scattering (Tables VII and VIII). The inclusion of $\overline{Q}$ space has a minor effect on the angular correlation parameter λ, but a large effect on R where CC (and CCO) do not predict the experimental sign change at about 80°. PP predicts small values of R from 60° to 100°, and differs markedly from CC in shape for $\theta > 50°$, although neither resembles the experimental trend qualitatively except for $\theta < 50°$. In fact differences in prediction of λ and R for large angles are difficult to consider, since no model works well. The largest effect of $\overline{Q}$ space for differential cross sections is on the $2s$ excitation (Table VII). We will pay particular attention to this as an indicator of the closeness of the dif-

TABLE III. The $1s$ angular distribution for e-H at 200 eV (a.u.). Numbers in square brackets indicate powers of 10. Figures in parentheses indicate the error in the last figure.

θ (deg)	Expt. (Ref. 8)	CCO	PP	PP2	BSSR
0		3.3	3.1	3.1	2.9
10		1.00	9.4[−1]	9.5[−1]	9.8[−1]
20	$4.2(4)\times10^{-1}$	4.0[−1]	3.9[−1]	3.8[−1]	3.8[−1]
30	$1.7(2)\times10^{-1}$	1.59[−1]	1.53[−1]	1.50[−1]	1.5[−1]
40	$7.1(7)\times10^{-2}$	6.5[−2]	6.5[−2]	6.3[−2]	6.2[−2]
60	$1.9(2)\times10^{-2}$	1.66[−2]	1.78[−2]	1.71[−2]	1.7[−2]
80	$8.6(9)\times10^{-3}$	6.2[−3]	6.8[−3]	6.5[−3]	6.5[−3]
100	$4.1(4)\times10^{-3}$	3.2[−3]	3.5[−3]	3.3[−3]	3.3[−3]
120	$2.7(4)\times10^{-3}$	1.91[−3]	2.1[−3]	2.0[−3]	2.0[−3]
140	$1.8(3)\times10^{-3}$	1.39[−3]	1.53[−3]	1.46[−3]	1.4[−3]
160		1.15[−3]	1.28[−3]	1.22[−3]	1.2[−3]

TABLE IV. The $2s$ angular distribution for e-H at 200 eV (a.u.). Numbers in square brackets indicate powers of 10.

θ (deg)	CCO	PP	PP2	BSSR
0	1.69	1.28	1.23	1.20
10	1.93[−1]	2.7[−1]	2.6[−1]	2.5[−1]
20	2.2[−2]	2.3[−2]	2.1[−2]	2.3[−2]
30	3.0[−3]	3.4[−3]	2.7[−3]	2.8[−3]
40	1.26[−3]	1.34[−3]	1.05[−3]	1.16[−3]
60	3.1[−4]	3.9[−4]	3.2[−4]	2.9[−4]
80	1.28[−4]	1.34[−4]	1.10[−4]	1.35[−4]
100	6.0[−5]	6.6[−5]	5.6[−5]	5.6[−5]
120	3.5[−5]	3.7[−5]	3.6[−5]	4.1[−5]
140	2.8[−5]	2.6[−5]	2.4[−5]	2.7[−5]
160	2.2[−5]	2.1[−5]	2.0[−5]	2.5[−5]

TABLE V. The $2p$ angular distribution for e-H at 200 eV (a.u.). Numbers in square brackets indicate powers of 10.

θ (deg)	CCO	PP	PP2	BSSR
0	2.1[+2]	2.1[+2]	2.1[+2]	2.5[+2]
10	1.56	1.45	1.42	1.46
20	4.3[−2]	2.9[−2]	2.6[−2]	2.4[−2]
30	2.4[−3]	2.2[−3]	1.36[−3]	1.6[−3]
40	8.1[−4]	7.9[−4]	5.6[−4]	5.2[−4]
60	1.96[−4]	2.2[−4]	1.79[−4]	2.0[−4]
80	1.02[−4]	1.08[−4]	9.6[−5]	1.08[−4]
100	6.3[−5]	6.4[−5]	6.0[−5]	6.6[−5]
120	4.7[−5]	4.6[−5]	4.6[−5]	6.0[−5]
140	3.8[−5]	3.7[−5]	3.8[−5]	4.7[−5]
160	3.4[−5]	3.2[−5]	3.4[−5]	5.1[−5]

TABLE VI. Cross sections (a.u.) for 54.42 eV e-H elastic scattering. Numbers in square brackets indicate powers of 10. Figures in parentheses indicate the error in the last figure.

θ (deg)	Expt. $\times 0.82$[a]	CCO	CC	PP	PP2	BSSR	PSO	PP2E	PPD
0		8.5	3.6	6.9	7.5	7.4	6.7	7.3	6.06
10	4.7(4)	3.9	1.98	3.3	3.7	3.8	3.0	3.6	2.7
20	9.8(2)	1.74	1.14	1.49	1.70	1.7	1.36	1.63	1.15
30	$9.0(8)\times10^{-1}$	9.2[−1]	7.2[−1]	7.8[−1]	8.7[−1]	8.9[−1]	7.5[−1]	8.5[−1]	5.7[−1]
40	$4.5(5)\times10^{-1}$	5.2[−1]	4.7[−1]	4.4[−1]	4.8[−1]	5.0[−1]	4.4[−1]	4.8[−1]	3.2[−1]
60	$1.7(2)\times10^{-1}$	1.8[−1]	1.96[−1]	1.77[−1]	1.70[−1]	1.8[−1]	1.85[−1]	1.88[−1]	1.36[−2]
80	$8.1(10)\times10^{-2}$	7.5[−2]	9.2[−2]	8.3[−2]	7.4[−2]	7.8[−2]	8.0[−2]	8.8[−2]	6.9[−2]
100	$4.6(6)\times10^{-2}$	4.3[−2]	5.1[−2]	4.6[−2]	4.1[−2]	4.1[−2]	4.3[−2]	4.8[−2]	4.1[−2]
120	$2.9(2)\times10^{-2}$	2.8[−2]	3.3[−2]	3.0[−2]	2.8[−2]	2.5[−2]	2.8[−2]	2.9[−2]	2.8[−2]
140	$2.2(2)\times10^{-2}$	2.1[−2]	2.5[−2]	2.3[−2]	2.2[−2]	1.8[−2]	2.1[−2]	1.93[−2]	2.3[−3]
σ_{1s}	3.83(40)[b]	3.25	2.53	2.91	3.11	3.18	2.78	3.12	2.31
σ_R	6.57(66)[b]	6.63	3.14	5.61	6.17	10.92	6.59	5.69	6.38

[a]50 eV.
[b]Actual value.

TABLE VII. Cross sections (a.u.) for $2s$ excitation of hydrogen at 54.42 eV. Numbers in square brackets indicate powers of ten. Figures in parentheses indicate the error in the last figure.

θ (deg)	Expt.	CCO	CC	PP	PP2	BSSR	PSO	PP2E	PPD
0		2.8	3.2	1.07	8.9[−1]	8.3[−1]	2.0	9.2[−1]	1.10
10	$3.8(13)\times10^{-1}$	4.3[−1]	5.8[−1]	2.5[−1]	1.88[−1]	1.6[−1]	3.0[−1]	1.92[−1]	2.4[−1]
20	$9.0(18)\times10^{-2}$	1.13[−1]	1.22[−1]	1.05[−1]	8.6[−2]	8.5[−1]	1.09[−1]	8.6[−2]	1.08[−1]
30	$3.5(4)\times10^{-2}$	3.0[−2]	4.4[−2]	3.4[−2]	2.5[−2]	2.5[−2]	4.2[−2]	2.7[−2]	3.7[−2]
40	$1.65(128)\times10^{-2}$	1.32[−2]	1.87[−2]	1.22[−2]	8.4[−3]	6.5[−3]	1.57[−2]	8.3[−3]	1.17[−2]
60	$1.01(48)\times10^{-2}$	7.9[−3]	1.01[−2]	5.9[−3]	4.9[−3]	4.2[−3]	6.2[−3]	3.3[−3]	4.2[−3]
80	$6.2(25)\times10^{-3}$	5.1[−3]	6.5[−3]	3.5[−3]	3.0[−3]	3.1[−3]	5.0[−3]	2.5[−3]	3.2[−3]
100	$3.9(11)\times10^{-3}$	3.5[−3]	4.5[−3]	2.2[−3]	1.86[−3]	2.1[−3]	2.9[−3]	2.4[−3]	2.6[−3]
120	$2.8(10)\times10^{-2}$	2.4[−3]	3.4[−3]	1.61[−3]	1.35[−3]	1.7[−3]	1.67[−3]	2.4[−3]	2.4[−3]
140	$2.2(9)\times10^{-3}$	1.82[−3]	3.0[−3]	1.40[−3]	1.14[−3]	1.5[−3]	1.23[−3]	2.4[−3]	2.4[−3]
σ_{2s}	0.166[a] 0.25[b]	0.25	0.32	0.167	0.131	0.124	0.21	0.135	0.169

[a]Kauppila *et al.*[14]
[b]Interpolation in data of Williams.[9]

TABLE VIII. Cross sections (a.u.) for 54.42-eV e-H $2p$ excitation. Numbers in square brackets indicate powers of 10. Figures in parentheses indicate the error in the last figure.

θ (deg)	Expt.	CCO	CC	PP	PP2	BSSR	PSO	PP2E	PPD
0		3.8[+1]	3.9[+1]	4.2[+1]	4.1[+1]	4.1[+1]	3.5[+1]	4.1[+1]	4.2[+1]
1	7.5(7)	7.6	7.8	7.6	7.3	7.4	7.4	7.3	7.9
20	1.04(11)	1.15	1.17	9.0[−1]	7.9[−1]	7.9[−1]	1.25	8.1[−1]	1.01
30	$1.57(21)\times10^{-1}$	1.68[−1]	1.97[−1]	1.22[−1]	8.3[−2]	7.8[−2]	2.1[−1]	9.5[−2]	1.36[−1]
40	$4.4(7)\times10^{-2}$	3.9[−2]	4.8[−2]	3.2[−2]	1.65[−2]	1.4[−2]	4.6[−2]	2.2[−2]	2.7[−2]
60	$1.19(21)\times10^{-2}$	1.01[−2]	1.13[−2]	9.9[−3]	6.0[−3]	6.1[−3]	1.15[−2]	8.2[−3]	7.8[−3]
80	$4.1(9)\times10^{-3}$	4.8[−3]	4.6[−3]	4.7[−3]	3.2[−3]	3.5[−3]	6.1[−3]	4.8[−3]	4.6[−3]
100	$2.2(5)\times10^{-3}$	2.5[−3]	2.6[−3]	2.5[−3]	2.0[−3]	2.0[−3]	3.4[−3]	2.5[−3]	2.9[−3]
120	$1.59(36)\times10^{-3}$	1.41[−3]	1.61[−3]	1.45[−3]	1.43[−3]	1.36[−3]	1.88[−3]	1.25[−3]	1.90[−3]
140	$1.03(28)\times10^{-3}$	9.5[−4]	1.25[−3]	8.6[−4]	1.06[−3]	8.4[−4]	1.32[−3]	1.03[−3]	1.31[−3]
σ_{2p}	2.79(24)	2.75	2.83	2.69	2.54	2.56	2.72	2.57	2.81

TABLE IX. $2p$ angular correlation parameter λ for 54.42-eV e-H scattering. Figures in parentheses indicate the error in the last figure.

θ (deg)	Expt.	CCO	CC	PP	PP2	BSSR	PSO	PP2E	PPD
0		1	1	1	1	1	1	1	1
10	0.34(5)	0.27	0.28	0.33	0.31	0.32	0.25	0.31	0.34
20	0.23(3)	0.187	0.192	0.26	0.189	0.20	0.159	0.21	0.25
30	0.55(4)	0.35	0.34	0.50	0.30	0.29	0.27	0.40	0.41
40	0.82(6)	0.72	0.68	0.89	0.73	0.67	0.59	0.83	0.81
60	0.92(6)	0.89	0.92	0.91	0.87	0.78	0.84	0.87	0.91
80		0.77	0.80	0.74	0.60	0.72	0.64	0.70	0.67
100	0.35(3)	0.80	0.80	0.60	0.40	0.76	0.77	0.60	0.57
120	0.53(4)	0.87	0.87	0.60	0.41	0.86	0.88	0.47	0.64
140	0.90(4)	0.94	0.96	0.82	0.59	0.95	0.94	0.34	0.84

ferent models. Note that neither CC nor PP obtain the detailed agreement with experiment that is obtained with CCO. The same is true for the $2p$ excitation (Table VIII), but this is dominated by the Born term (at least at forward angles) and is therefore less sensitive to models for Q space.

Two basic methods have been suggested for reducing the amount of computational labor involved in a coupled-channels calculation with a pseudostate representation of Q space. One is to ignore exchange in a coupled-channels calculation.[7] This is tested by comparing PPD with PP. For the elastic channel PPD cross sections are considerably smaller in the middle angular range. For $2s$ and $2p$ there are serious differences near 60° and at large angles. Differences for λ and R are small, indicating (perhaps surprisingly) that these coefficients are insensitive to the omission of exchange.

Other proposed methods for reducing computation all rely on treating $\bar{Q}$ space in second order. PP2E makes only this approximation. In general it overestimates elastic cross sections, but is closer to PP than PPD (which underestimates them). It is a much worse approximation for $2s$ than PPD, where it underestimates cross sections considerably, and it is roughly comparable for $2p$. For λ and R, PP2E is a worse approximation than PPD.

PP2 makes one more approximation than PP2E. It omits exchange from couplings to $\bar{Q}$ space but retains it within P space. For elastic scattering it is not very different from PP2E. It is comparable to PP2E for small angles in the $2s$ channel but seems to make compensating errors in the 60°–80° range. For $2p$ it provides worse underestimates of PP than does PP2E up to 100°. For λ at small angles it enhances the errors of PP2E (but fortuitously is much closer to the experimental minimum at large angles). For R up to 60° it is comparable with PP2E. The worst (and probably unacceptable) feature of PP2 is its serious underestimate of middle-range inelastic cross sections.

The other methods BSSR and PSO are polarization potential approximations to PP2 and PP2E, respectively. BSSR is a coordinate-space method which does not make the equivalent local approximation used in PSO. BSSR omits exchange from $P\bar{Q}$ couplings whereas PSO includes it. PSO computes polarization potentials in momentum space.

BSSR should be considered as an approximation to PP2. Comparisons are made in Figs. 1–4 as well as in the tables. The two calculations are quite similar for differential cross sections and for small-angle values of λ and R, but are entirely different for λ and R at large angles. The difference is surprisingly large for σ_R.

For elastic scattering PSO is a reasonable approximation to PP2E, but for the inelastic features it is nearer to CC than to PP2E, indicating that the momentum-space calculation of polarization potentials for $\bar{Q}$ space is an underestimate. This is somewhat surprising, since the method works well for real $n=3$ states in comparison with a six-state CCO model.[21]

At 200 eV we have calculated PP2 and BSSR for comparison with PP (Tables II–V). For elastic cross sections all models give similar results. BSSR is a reasonably good approximation to PP2 for $2s$ cross sections, but both un-

TABLE X. $2p$ angular correlation parameter R for 54.42-eV e-H scattering. Figures in parentheses indicate the error in the last figure.

θ (deg)	Expt.	CCO	CC	PP	PP2	BSSR	PSO	PP2E	PPD
0		0	0	0	0	0	0	0	0
10	0.28(3)	0.30	0.30	0.33	0.33	0.33	0.29	0.32	0.33
20	0.21(2)	0.22	0.22	0.27	0.26	0.27	0.22	0.26	0.29
30	0.18(2)	0.23	0.23	0.25	0.25	0.26	0.24	0.25	0.27
40	0.122(18)	0.21	0.22	0.166	0.195	0.22	0.28	0.20	0.17
60	0.082(3)	0.103	0.110	0.011	0.056	0.19	0.21	0.070	−0.025
80		0.146	0.100	−0.014	−0.000	0.20	0.23	0.038	−0.002
100	−0.113(33)	0.173	0.158	0.027	0.081	0.20	0.24	0.050	0.092
120	−0.065(30)	0.160	0.190	0.161	0.194	0.18	0.183	0.081	0.178
140	−0.056(40)	0.118	0.118	0.184	0.26	0.12	0.116	0.22	0.191

derestimate PP in the middle angular range. This is true also at 54.42 eV. For the $2p$ excitation PP2 underestimates PP, as it also does at 54.42 eV, but BSSR overestimates PP2 at most angles. Angular correlation parameters are not shown at 200 eV, since there is no reliable experimental information.

IV. CONCLUSIONS

The coupled-channels optical model agrees well with most experimental data for the $1s,2s,2p$ P space at 54.42 and 200 eV, although at 54.42 eV it differs from experimental values by more than one standard deviation for some Q-space features. At 200 eV the model represents total cross sections for Q-space excitations very well. The notable exception for P space is the CCO description of the $2p$ angular correlation parameters λ and R for $\theta > 60°$, where it may be several standard deviations outside the experimental error limits. Nevertheless it describes λ and R better in general than the other models. This model represents Q space by polarization potentials involving explicit integration of products of approximate amplitudes over the appropriate kinematic degrees of freedom.

The pseudoproblem in which Q space is represented by a set ($\bar{Q}$ space) of seven pseudostates, gives a description of P-space features at both energies that is very similar to CCO. The only noticeable differences are the $2s$ differential cross section at 54.42 eV, where it underestimates the experiment significantly and the angular distribution of λ at 54.42 eV, where it is closer to the experimental data than CCO. The pseudostates are chosen to fit the dipole polarizability and some low-energy P-space features. They underestimate σ_Q by over 20% at both energies, where experimental standard deviations are about 10%.

There is no doubt that a larger set of pseudostates can be found that will give a better solution to the e-H problem than the present seven-pseudostate set. It will be difficult to solve all the coupled equations explicitly for such a set. We have therefore investigated some approximate solutions for the present set in anticipation of applying them to an improved set in the future.

The approximation (PPD) of solving the coupled equations explicitly with total neglect of exchange is, perhaps surprisingly, good at 54.42 eV and would be better at 200 eV where exchange terms are smaller.

The approximation that is most attractive in terms of saving computational labor is the use of second-order polarization potentials representing $\bar{Q}$ space in the P-space coupled-channels calculation. We have investigated a coordinate-space calculation (BSSR) and an equivalent local momentum-space calculation (PSO) in comparison with coupled-channel calculations (PP2 and PP2E) in which only the second-order approximation is made. PP2 and PP2E omit and include $P\bar{Q}$ exchange amplitudes, respectively. In general second-order approximations give fairly serious underestimates of $2s$ and $2p$ cross sections at both energies, when compared with PP. BSSR is a good approximation to PP2 for differential cross sections, but breaks down badly for the total reaction cross sections and the angular correlation parameters at 54.42 eV. The momentum-space calculation PSO is not a sufficiently accurate approximation to PP2E to be considered without some refinement as a good alternative to BSSR.

Finally we consider what we have learned about possible improvements to these calculations. CCO could be improved by going beyond the screened second-order approximation to $\Psi_\mu^{(-)}$ in Eq. (1) for the polarization potential. Distorted-wave calculations of amplitudes are not difficult, but are extremely time consuming and impractical in the integrand of the multidimensional kinematic integral. CCO is a good approximation, but difficult to improve.

PP can be improved by finding a set of pseudostates that gives an improved representation of the Q-space features of the hydrogen atom. The difficulty here is to solve the large set of coupled equations involved. Second-order methods do not give a very good approximation to the present pseudoproblem and therefore would not be expected to do better for an improved pseudoproblem.

The use of an L^2 expansion to represent the three-body wave functions $\Psi_\mu^{(-)}$ in a polarization potential must go beyond the second order. This means that we need an L^2 expansion in three-body space, not merely in the two-body space of the target.

ACKNOWLEDGMENTS

We would like to acknowledge financial support from the Australian Research Grants Scheme. One of us (B.H.B.) acknowledges travel support from the Royal Society and the University of Durham.

[1]I. E. McCarthy and A. T. Stelbovics, Phys. Rev. A **22**, 502 (1980).
[2]I. E. McCarthy and A. T. Stelbovics, Phys. Rev. A **28**, 2693 (1983).
[3]B. H. Bransden and A. T. Stelbovics, J. Phys. B **17**, 1877 (1984).
[4]B. H. Bransden, T. Scott, R. Shingal, and R. K. Roychoudhury, J. Phys. B **15**, 4605 (1982).
[5]J. Callaway and J. W. Wooten, Phys. Rev. A **9**, 1924 (1974).
[6]I. E. McCarthy and A. T. Stelbovics, Aust. J. Phys. **36**, 665 (1983).
[7]L. A.Morgan, J. Phys. B **15**, 4247 (1982).
[8]J. F. Williams, J. Phys. B **8**, 2191 (1975).
[9]J. F. Williams, J. Phys. B **14**, 1197 (1981).
[10]S. T. Hood, E. Weigold, and A. J. Dixon, J. Phys. B **12**, 631 (1979).
[11]E. Weigold, L. Frost, and K. J. Nygaard, Phys. Rev. A **21**, 1950 (1980).
[12]B. van Wingerden, E. Weigold, F. J. de Heer, and K. J. Nygaard, J. Phys. B **10**, 1345 (1977).
[13]I. E. McCarthy and A. T. Stelbovics, Aust. J. Phys. **34**, 135 (1981).
[14]W. E. Kauppila, W. R. Ott, and W. L. Fite, Phys. Rev. A **1**, 1099 (1970).

[15]F.J. deHeer, M. R. C. McDowell, and R. W. Wagenaar, J. Phys. B **10**, 1945 (1977).
[16]W. L. Fite and R. T. Brackmann, Phys. Rev. **112**, 1141 (1958).
[17]A. H. Mahan, A. Gallagher, and S. J. Smith, Phys. Rev. A **13**, 156 (1976).
[18]R. L. Long, D. M. Cox, and S. J. Smith, J. Res. Natl. Bur. Stand. Sect. A **72**, 521 (1968).
[19]B. H. Bransden and M. R. C. McDowell, Phys. Rep. **46**, 249 (1978).
[20]B. Lohmann, I. E. McCarthy, A. T. Stelbovics, and E. Weigold, Phys. Rev. A **30**, 758 (1984).
[21]I. E. McCarthy and A. T. Stelbovics, J. Phys. B **16**, 1611 (1983).